CONF-961005--20

GA–A22476

DISRUPTION STUDIES IN DIII–D

by
A.G. KELLMAN, J.W. CUTHBERTSON, T.E. EVANS,
D.A. HUMPHREYS, A.W. HYATT, G.L. JAHNS,
T. JERNIGAN, C.J. LASNIER, R.L. LEE, J.A. LEUER,
S. LUCKHARDT, M.J. SCHAFFER, P.L. TAYLOR,
D.G. WHYTE, D. WRÒBLEWSKI, and J. ZHANG

SEPTEMBER 1996

GENERAL ATOMICS

DISCLAIMER

GA–A22476

DISRUPTION STUDIES IN DIII–D

by
A.G. KELLMAN, J.W. CUTHBERTSON,* T.E. EVANS,
D.A. HUMPHREYS, A.W. HYATT, G.L. JAHNS,†
T. JERNIGAN,‡ C.J. LASNIER,Δ R.L. LEE, J.A. LEUER,
S. LUCKHARDT,* M.J. SCHAFFER, P.L. TAYLOR,
D.G. WHYTE,# D. WRÒBLEWSKI,† and J. ZHANG#

This is a preprint of a paper to be presented at the Sixteenth IAEA International Conference on Plasma Physics and Controlled Nuclear Research, October 7–11, 1996, Montreal, Canada, and to be published in *The Proceedings.*

*University of California, San Diego, California.
†ORINCON Corporation, San Diego, California.
‡Oak Ridge National Laboratory, Oak Ridge, Tennessee.
ΔLawrence Livermore National Laboratory, Livermore, California.
#INRS — Energie et Materiaux, Varennes, Quebec, Canada.

Work supported by
the U.S. Department of Energy under Contract Nos.
DE-AC03-89ER51114, DE-AC05-96OR22464, W-7405-ENG-48,
and Grant No. DE-FG03-95ER54294

GA PROJECT 3466
OCTOBER 1996

GENERAL ATOMICS

F1-CN-64/AP1-20

DISRUPTION STUDIES IN DIII–D

ABSTRACT

Characteristics of disruptions in the DIII–D tokamak including the current decay rate, halo current magnitude and toroidal asymmetry, and heat pulse to the divertor are described. Neon and argon pellet injection is shown to be an effective method for mitigating the halo currents and the heat pulse with a 50% reduction in both quantities achieved. The injection of these impurity pellets frequently gives rise to runaway electrons.

1. INTRODUCTION

Disruptions represent a serious obstacle to the successful realization of a commercially viable tokamak power plant. In addition to the high thermal and electromagnetic loads resulting from the rapid loss of both thermal and magnetic energy, disruptions can generate large, toroidally asymmetric poloidal "halo" currents in the scrapeoff layer. These currents strongly influence tokamak design because they can give rise to large forces on the vessel and internal components. This paper describes work on the DIII–D tokamak on the characterization of these different disruption phenomena, successful reduction of the heat pulse and halo currents using neon and argon pellets, and the development of a real time disruption avoidance system for high beta discharges using a neural network.

2. DISRUPTION CHARACTERIZATION

Disruptions in DIII–D fall into two basic classes, major disruptions and vertical displacement events (VDEs). In a major disruption, an MHD mode grows, leading to a loss of thermal energy (thermal quench) and the resulting cold plasma suffers a rapid decay of the plasma current (current quench). In single null divertor discharges, a loss of vertical position in the direction of the X–point typically follows the thermal quench. In a VDE, the loss of vertical position precedes the thermal quench. As the plasma moves vertically against the first wall, the cross section and edge q decrease until the shrinking plasma disrupts, losing its thermal energy, typically when the edge q approaches two.

For both disruption types, a rapid decay in the plasma current is observed following the thermal quench. Although there is a large variation in the current decay rate for a given plasma current, for full aperture discharges (volume>19m^3) the fastest current decays have a characteristic decay time, $I_{po}/(dI/dt) \sim 4$ ms, where I_{po} is the pre-disruption current and dI/dt is the average decay rate from 90% to 10% of the current. VDEs have the shortest decay times because the dual effects of the reduced cross section and the high resistivity of the cold plasma increase the plasma resistance. Discharges with low plasma current, small volumes (<15 m^3) and large distances to the conducting wall exhibit even shorter decay times, approaching 2 ms. The post-thermal quench equilibria for these discharges are so vertically unstable, that they exhibit extremely rapid loss of vertical position and have shorter decay times than full-aperture VDEs.

Heat flux measurements during disruptions show that the relative importance of two energy loss mechanisms, conduction to the divertor floor and radiation, depend on the type and phase of the disruption. In three different disruptions, the fraction of the total energy lost during the thermal quench (primarily the thermal energy) that was conducted to the floor varied considerably: 85% for a VDE, 50% for a major disruption at high beta and 22% for a discharge terminated by a large argon puff. During the thermal quench, radiation plays a very small role in a VDE while it dominates the energy loss in the argon puff disruption. In all cases, the role of radiation increases in the current quench phase and is the major energy loss mechanism. In the VDE and the argon puff disruptions, radiation accounts for 85%–90% of the energy lost during the current quench with a value of 65% for the high beta disruption. Detailed heat flux measurements and a complete energy balance during DIII–D disruptions have been reported earlier by Lee [1] and Hyatt [2].

One of the more significant disruption-related problems for future machines is the development of large poloidal currents that flow on the open field lines surrounding the plasma and return poloidally through the vessel. These poloidal "halo" currents interact with the toroidal field resulting in large, poloidally localized forces on the vessel and internal components [3]. In order to better understand the driving mechanism and dependence of the halo current on plasma properties, we have conducted a series of experiments in which a VDE is initiated by disabling the vertical feedback system. The poloidal and toroidal structures of the poloidal halo currents are measured with an extensive array of detectors in the lower divertor region referred to as the tile current array (TCA) [4].

The basic phenomenology of the VDE is shown in Fig. 1. As the plasma drifts vertically downward [Fig. 1(a)], its cross section shrinks, the edge safety factor decreases, and the plasma disrupts, losing its thermal energy [Fig. 1(b)]. During the VDE, two mechanisms drive the halo current. Following the thermal quench, the core plasma current (that contained within the last closed flux surface) begins to decay, inducing toroidal current in the cold "halo" plasma on the open field lines surrounding the last closed flux surface [Fig. 1(c)]. Flux contours and toroidal halo current are determined using an array of distributed current elements to represent the plasma and calculating the best distribution of currents in the plasma region and vessel to fit magnetic diagnostics. Because the halo region is essentially force free ($jxB=\nabla p\sim 0$), the current flows along the field lines. Thus by driving a toroidal halo current, a poloidal current is also driven that is related to the toroidal component by $I_{halo}(pol) = I_{halo}(tor)/q_{edge}$ [Fig. 1(d)]. A second mechanism that directly drives poloidal halo current is the reduction in the toroidal flux linked by the plasma as the cross section shrinks. Comparison of the two driving terms shows that at the time of maximum poloidal halo current, the driving voltage from the current decay, $V_{dI/dt}$, is considerably larger than that from toroidal flux compression, $V_{d\phi/dt}$, although the terms are comparable earlier in the buildup of the poloidal current [Fig. 1(e)]. The halo width increases as the plasma moves downward and at the time of the peak poloidal halo current the halo width is typically 10–15 cm, measured on the plasma midplane. During the final stage of the current decay, there are no closed flux surfaces and all the toroidal current is carried on open field lines. Despite the finite toroidal halo current (I_{halo}(toroidal)=420 kA at 1.7275 s), the poloidal halo current is very small during this stage because the edge q is very high.

Poloidal halo currents of up to 30% of the pre-disruption current, I_{po}, have been measured during VDE's when the data is averaged over ± 0.5 ms (Fig. 2). Values up to 40% have been observed with shorter averaging (± 0.1 ms). The scaling proposed by Granetz [5], $I_{halo}/I_{po}\sim 1/q_{950}$, ($q_{950}$ is the pre-disruption q at the 95% flux surface) does not explain the DIII–D data in which large variations in halo current are observed at

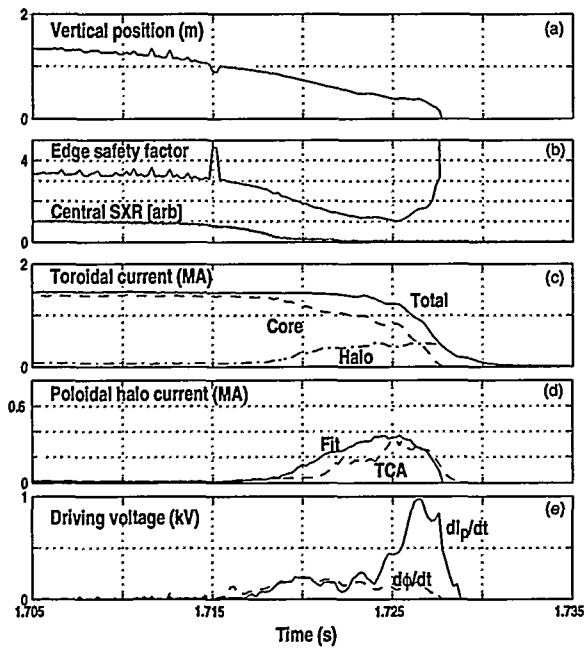

Fig. 1. Time evolution of a VDE (β_n=1.1, shot 90219). Poloidal halo current reaches 370 kA (23% of the pre-disruption I_p). The peak poloidal halo current determined by a magnetic fitting code (FIT) agrees well with that measured by the tile current array (TCA).

fixed I_{po}/q_{950} and the highest halo current is observed at high q_{95}. Examination of two discharges with the same I_{po} and q_{950} but a factor of two difference in I_{halo}/I_{po} (23% vs. 10%) is useful to understand the underlying physics determining the magnitude of the halo current.

I_p=1.48MA,q_{950}=3.4	I_{halo}/I_{po}	dI_p/dt(core)	I_{halo}(tor)	$q$edge-min
low βn=1.1	0.23	150 MA/s	0.46 MA	1.00
high βn=3.2	0.10	670 MA/s	0.62 MA	2.05

Because $I_{halo}(pol)=I_{halo}(tor)/q_{edge}$, if a sufficiently high edge q is maintained during the VDE evolution, a low poloidal halo current will result even if a large toroidal halo current is driven by the current decay in the plasma core. An analytic model shows that a key parameter determining the evolution of the edge q and thus the halo current evolution is the quantity γ_p/γ_z where γ_p is the initial plasma current decay rate and γ_z is the vertical instability growth rate. Since $q_{edge}\sim a^2/I_p$ (a is the minor radius), a rapid current decay relative to the instability growth rate (γ_p/γ_z >1) results in a high edge q because the current decays while the plasma cross section is still large ($q_{edge\text{-}min}$=2.05) This is the case for the high beta discharge shown in the table. In the opposite regime, γ_p/γ_z <1, a slow current decay relative to the vertical motion allows the edge q to get small ($q_{edge\text{-}min}$=1.0) and thus even for lower toroidal halo current, the poloidal halo current is larger. This is the case for the low beta discharge. This implies that a successful technique to reduce poloidal halo currents is to induce a rapid current decay while the plasma is still far from the floor and large enough to have a high edge q. The impurity pellet injection described in the next section follows this approach.

The critical consequence of the poloidal halo currents is the resulting vertical force on the vessel. On DIII–D, the force is inferred from direct measurement of the vertical

vessel displacement. This is shown to scale linearly with poloidal halo current magnitude as expected since the duration of the halo current is short compared to the characteristic mechanical times of the vessel.

In addition to the large amplitude of the halo currents, large toroidal asymmetries are observed in the halo current. Toroidal peaking factors (peak-to-average value) as high as 3 are observed at the time of peak halo current with values as high as 5 for shorter averaging times, ±0.1 ms (Fig. 2). As shown in the figure, a value of I_{halo}/I_{po} of 30% with a 2:1 toroidal peaking factor represents the highest combination obtained simultaneously at the time of the peak halo current. Typically, the maximum halo current occurs near the minimum peaking factor for a given discharge. Often however, at only slightly reduced halo current, the peaking factor is considerably higher. This is shown by the curve in Fig. 2 (labeled no pellet) which represents the trajectory of one discharge (I_{halo}/I_{po} vs. peaking factor). The shaded region represents the boundary of the trajectories for all discharges studied.

The toroidal structure of the halo current can be highly localized with a non-sinusoidal perturbation that is less than 100° in toroidal extent. However, asymmetries are also observed that more closely resemble an n=1 sinusoidal structure. Rotation of the asymmetry is always observed during the initial phase of the VDE when the discharge is drifting vertically prior to the thermal quench. Typical rotation frequencies are 200–400 Hz and the structure generally rotates opposite to the bulk plasma rotation. The asymmetry typically continues to rotate following the thermal quench, however, locking has been observed. When the asymmetry locks, there is no preferred toroidal location for the locking. The implication of the locking is that toroidally discrete components in the vessel effectively see higher poloidal currents than if the asymmetry rotated and the force was averaged over a large toroidal extent.

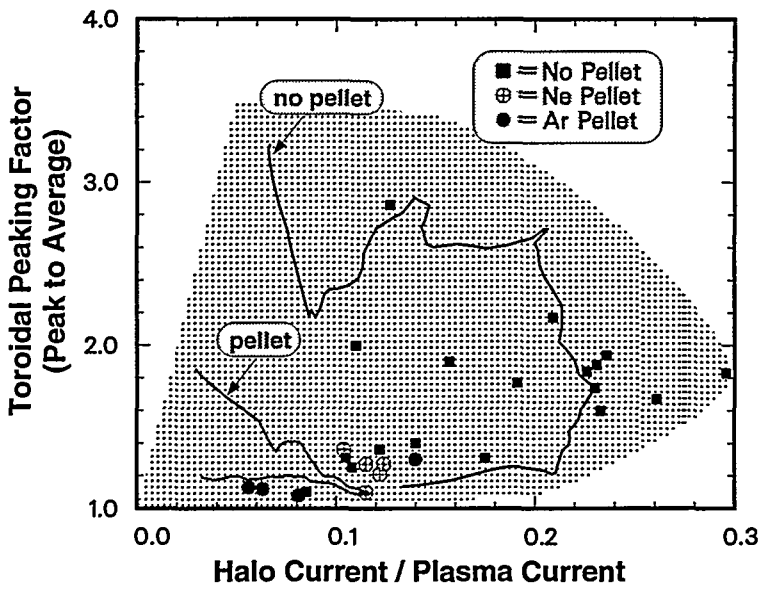

Fig. 2. Toroidal peaking factor and halo current normalized to the pre-disruption plasma current for VDEs. Points show the values at the time of peak halo current. The two solid lines show the trajectory of a pellet and non-pellet discharge with identical pre-disruption equilibria. The shaded region is the boundary of the trajectories of all discharges.

3. DISRUPTION MITIGATION AND AVOIDANCE

The combined effects of high halo currents, toroidal asymmetries in the halo currents, and the intense heat pulse during the disruption make mitigation of disruptions imperative. In DIII–D we have explored the use of both neon and argon pellet injection and have shown that both are effective at significantly reducing these effects. In our experiments, these pellets were injected both into VDEs and into centered, well controlled discharges in order to test pre-emptive termination of discharges. The pellet injector uses high pressure He gas as a propellant and two different size pellets (1.7 mm and 2.8 mm) were tested in these experiments. The 2.8 mm Ne pellets contained 3×10^{20} Ne atoms which represented approximately 35% of the electron content of the discharges. Depending on the vertical position of the plasma at the time of injection and the pellet size and speed, penetration varied from ρ/a of 0.55 to 0.25, where ρ/a is the normalized flux coordinate.

The basic phenomenology of pellet injection into a VDE is shown in Fig. 3. In this discharge, a 2.8 mm argon pellet is injected after the beginning of the vertical instability when the discharge is 15 cm below its nominal equilibrium position [Fig. 3(a)]. The duration of the ablation is 600 μs and the current decay begins within 200 μs of the end of the ablation. The stored energy loss begins promptly with the pellet injection and is complete within 100–200 μs of the end of the ablation [Fig. 3(b)]. During the 600 μs ablation, the internal inductance of the current profile increases from 0.75 to 1.0. The pellet causes the growth of large n = 1 and n = 2 modes [Fig. 3(d)] which may play a role in the loss of the remaining thermal energy and the subsequent profile flattening indicated by the drop in ℓ_i.

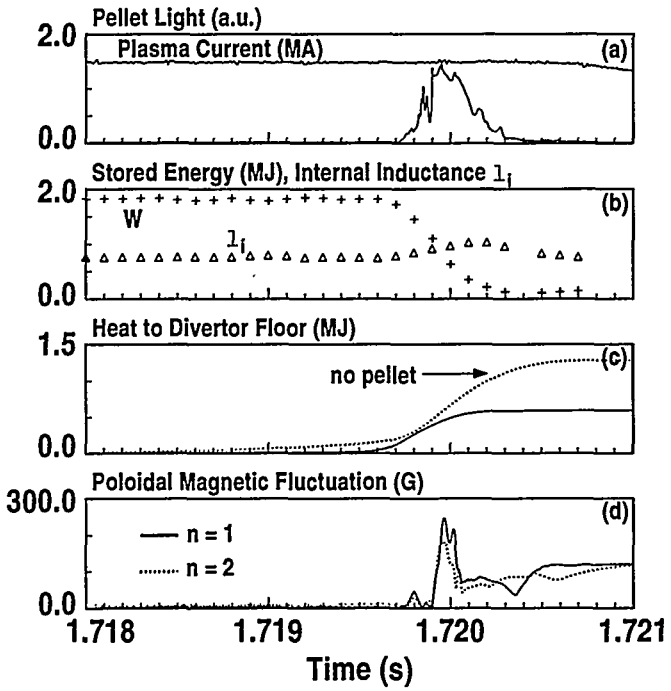

Fig. 3. Argon pellet injection into a VDE (β_n=3.2, q=3.4, shot 90206) causes an immediate loss of stored energy and rapidly initiates the current quench. The heat conducted to the floor is reduced by 50% with the injection of a pellet. Large MHD activity develops within 250 μs of pellet injection.

Both the Ne and Ar pellets were successful at significantly reducing the halo current magnitude and toroidal asymmetry during a VDE (Fig. 2). Typical reduction of the halo current was 30%–50% with the largest percentage reductions for the highest halo currents. The peaking factors were reduced to below 1.4 on all pellet discharges with typical values of 1.1–1.2. Moreover, the reductions in both magnitude and peaking factor are observed throughout the entire disruption, not just at the time of peak halo currents, as shown by the trajectory curves for the pellet and the non-pellet discharges in Fig. 2. Mitigation was successful over the full range of q_{95} values tested, 2.7 to 4.0, and with both small and large pellets. For both Ne and Ar pellets, injecting pellets into a well centered discharge led to the lowest halo currents and lowest vessel displacement with 65% lower halo current than a comparable VDE. There are two primary reasons for the effective halo current reduction with pellet injection. The higher current decay rate due to the higher resistivity with the pellet injection and the early injection of the pellet combine to make the current decay while the plasma has a larger cross section. This keeps the q high and, as described earlier, results in a low poloidal halo current.

Analysis of IR camera data from the Ne and Ar killer pellet experiments has clearly shown at least a 50% reduction of the disruption heat pulse to the divertor floor. Using an Ar pellet injected into a VDE, the total energy conducted to the divertor region during the thermal quench was only 30% of the thermal energy compared to 62% for the comparable VDE [Fig. 3(c)]. Similarly, when the combined thermal and current quench phases are considered, only 16% of the total energy available (thermal and magnetic energy) was conducted to the divertor compared with 38% for the comparable VDE. Heat flux mitigation has also been observed with neon injection where less than 20% of the energy lost during the thermal quench was conducted to the divertor region.

Although the heat flux mitigation to the divertor is not complete, the discharge shown in Fig. 3 (β_n=3.2, q_{95}=3.4) demonstrates that the use of pellet injection is a viable method for high beta discharges near the stability limit. In this discharge, both the n=1 and n=2 modes grow to ~200 G within 250 μs after the start of pellet injection. Despite this, the energy loss due to radiation from the pellet is so large and rapid that the plasma stored energy has decreased by ~50% before the MHD grows. In lower β discharges, the impurity radiation decreases the stored energy by more than 75% of its initial value before any MHD activity grows. Although we have no measurements of the energy conducted to the divertor on these discharges, the prompt loss of the thermal energy before the rise of MHD activity indicates that the heat flux mitigation due to radiation is more complete at lower β when the plasma is farther from the stability boundary.

The rapid and effective loss of thermal energy with the pellet injection is confirmed by a 1-D model of the plasma including pellet ablation and impurity radiation (conduction is not included). The model predicts that at ρ/a =0.7, the peak radiated power occurs within 20 μs after the Ne pellet is ablated and within 150 μs, both the electron and ion temperatures at that radius are at 10 eV ($T_{initial}$ ~ 2 keV). The high electron density following the pellet injection accounts for the effective coupling of the ion and electron temperature (T_e). Measurements of T_e using a multi-pulse Thomson scattering system confirm model predictions of 5–10 eV for $0.5 < \rho/a < 0.9$ with slightly higher temperatures near the plasma edge because the neon is deposited predominantly inside ρ/a=0.9. Both the model and measurements of the Ne spectrum show that the plasma cools so rapidly that no charge states above Ne^{+8} are produced.

Despite the successful mitigation of halo current and heat flux, a critical problem created by the pellet injection is the formation of runaway electrons. Evidence of runaway electrons was observed as single or repeated bursts of hard X–rays and by non-thermal ECE emission following the pellet ablation and often throughout the current decay phase. Runaways were observed on every discharge with Ar pellets and many Ne pellets. No runaway electron signatures were observed on any of the non-pellet VDEs.

A critical part of the DIII–D program is identification of the disruption boundary so that either the disruption can be avoided or a mitigation technique can be implemented. To accomplish this, an artificial neural network, combining a large set of plasma diagnostic signals has been implemented on DIII–D to estimate the high β disruption boundary [6]. A sensitivity analysis was used to reduce the set to 33 signals of importance, including poloidal field and flux, diamagnetic flux, magnetic fluctuations, D_α, soft X–ray, visible bremsstrahlung, and neutron emission, and line averaged density. The system has been implemented in real-time on the DIII–D control system and is operated routinely. The network more accurately predicts the disruption boundary than the usual formulation (β_{max}~I/aB) and can correctly predict the disruption boundary more than 100 ms in advance of the disruption.

4. SUMMARY

The current decay rate, heat flux to the divertor, and halo current magnitude and structure have been measured during disruptions in DIII–D. Halo currents up to 30% of the pre-disruption plasma current with a toroidal peaking factor of 2:1 have been observed during VDEs and the magnitude depends on the current decay rate relative to the vertical instability growth rate. Neon and argon pellet injection into these VDEs has been effective at reducing the halo currents by 50%, almost eliminating the toroidal asymmetry, and reducing the heat flux conducted to the divertor by at least 50% in reactor relevant discharges (q=3.4, β=3.2). A serious consequence of this impurity pellet injection technique is the formation of runaway electrons. A real-time neural network technique has been developed that predicts the high β disruption boundary sufficiently in advance of the disruption to make mitigation or avoidance schemes feasible.

REFERENCES

[1] LEE, R.L. *et al.*, "Thermal Deposition Analysis During Disruption on DIII–D Using Infrared Scanners," in Proc. 16th Symp. on Fusion Engineering, Vol. 2 (1996) p. 902.

[2] HYATT, A.W., et al., "Magnetic and Thermal Energy Flow During Disruptions in DIII–D," in Proc. 23rd Euro. Conf. on Contr. Fusion and Plasma Physics, Kiev, Ukraine, 1996 (European Physical Society, Petit-Lancy, Switzerland) to be published.

[3] STRAIT, E.J., and LAO, L.L., Nucl. Fusion **31** 527 (1991).

[4] EVANS, T.E., et al., "Measurements of Non-Axisymmetric Halo Currents With and Without "Killer" Pellets During Disruption in the DIII–D Tokamak," in Proc. 12th Int. Conf. on Plasma Surface Interactions in Contr. Fusion Devices, St Raphael, France , 1996, to be published in J. Nucl. Mater.

[5] GRANETZ, R., et al., Nucl. Fusion **36** 545 (1996).

[6] WROBLEWSKI, D., et al., "Tokamak Disruption Alarm Based on a Neural Network Model of the High Beta Limit," submitted to Nucl. Fusion.